Monte Carlo dynamics of a dense system of chain molecules constrained to lie near an interface. A simplified membrane model

Mariusz Milik
Technical University of Radom, Chrobrego 45, 26-600 Radom, Poland

Andrzej Kolinski
Department of Chemistry, University of Warsaw, Pasteura 1, 02-093, Warsaw, Poland

Jeffrey Skolnick[a)]
Department of Molecular Biology, Research Institute of Scripps Clinic, 10666 North Torrey Pines Road, La California 92037

(Received 9 March 1990; accepted 8 June 1990)

The static and dynamic properties of a dense system of flexible lattice chain molecules, one of whose ends is constrained to lie near an impenetrable interface, have been studied by means of the dynamic Monte Carlo method. It is found that increasing the surface density of the chains in the layer increases the orientational order. The value of the order parameter of the chain segments decreases with increasing distance from the interface. The short time dynamics of the model chains are similar to those observed in polymer melts. Then, there is a time regime of strongly hindered collective motion at intermediate distance scales. Finally, for distances greater than the chain dimensions, free lateral diffusion of the chains is recovered. It is shown that the model exhibits many features of the real systems such as detergents on a surface and lipid bilayers.

I. INTRODUCTION

The model system considered in the present work consists of a collection of chain molecules that are terminally adsorbed to a planar interface. The absorbed head of each chain in the system is allowed to move freely in the direction parallel to the interface and can bob slightly up and down in the direction perpendicular to the interface. Consequently, lateral diffusion of the entire chain is possible. Since chains essentially cannot diffuse in the direction orthogonal to the interface, the time average density of the chain segments at a given distance from the interface is strictly preserved.

A similar set of restrictions of the dynamics applies to the motion of the chain molecules found in a large micelle and when the detergents are on a surface.[1] Presumably, this is also the situation that may be found when one focuses attention on one side of a lipid bilayer.[2-4] Therefore, even qualitative insight into the mechanism of the conformational rearrangements and chain diffusion seems to be important; it would provide a better understanding of the large spectrum of phenomena observed in these motionally and orientationally anisotropic systems.

The model chains are restricted to a diamond (tetrahedral) type lattice. This is the lattice representation of the rotational isomeric states model[5] (RISM) of the conformation of alkane chains. Monte Carlo dynamics[6] (MCD) are used to model the chain motion in the layer. The reasons for employing these simplifications are the following: First, it has been shown for various polymer systems that the lattice representation works very well when applied to the study of equilibrium properties.[7-11] It is, also, qualitatively correct for modeling the dynamics of dense polymer systems, although the time scale for very local processes can be somewhat distorted in comparison to the real time scale.[11,12] Second, while there is substantial work on lattice models of a single polymer (or oligomer) chain absorbed onto an interface,[13-17] there are few studies on the static properties of lattice multichain systems with an absorbing surface. Over a comparable range of model parameters, the lattice approximation[14] leads to the similar results as the computationally far more intensive off-lattice simulations.[17-19] Thus, the nature of the dynamics of these systems and the possible correlation between the static and dynamic properties seems to be worth exploring. Finally, use of a lattice representation and the application of MCD makes the task computationally tractable. Since we are also interested in large scale displacements of dense multichain systems, a more exact molecular dynamics study of the detailed model would be extremely expensive on contemporary computers. Typically, a molecular dynamics (MD)[20] or a Brownian dynamics (BD)[21] study of the lipid bilayer covers a time scale corresponding to very local relaxations of the system configuration. Thus, the present simulations may be viewed as complementary to the more detailed MD and BD studies.[20,21] At the expense of introducing the simplifications discussed above, we are attempting to obtain a qualitative picture of the character of the long distance dynamics. On the other hand, all the effects related to the excluded volume, local geometry, and topological restrictions on the chain conformation and dynamics should be qualitatively the same, regardless of the model of local dynamics used. Of course, there are specific requirements for the MCD scheme, which solves a Master equation for the motion of the system under consideration.

The present model is athermal. Only hard core, excluded volume interactions between the chain segments are taken into account. As a result, the behavior of the system is temperature independent, except for the trivial contribution of the temperature to the frequency of elementary jumps,

a) To whom correspondence should be addressed.

 0021-9606/90/184440-07$03.00

which defines the time scale of MCD (or rather the relationship between MCD time and the time scale of the real processes that are modeled). Therefore, the polymer–polymer interactions correspond to the case of a good solvent surrounding the oligomer layer. Since the systems studied are quite dense, this assumption does not exert too large of an effect on the dynamics. Hence, the results of the simulations can be considered relevant to the more general situation than merely to the case of a strictly athermal system.

II. METHOD OF SIMULATION

The model system consists of N chains of the same length n. Hence, every chain the system occupies $n = 17$ diamond lattice points (chain beads), separated down the chain by a bond vector of type ($\pm 1, \pm 1, \pm 1$). The tetrahedral valence angle is preserved, and three rotational isomeric states (one trans and two gauche states) are allowed for three successive bonds. As a result, the model chains are flexible and can appear in a large number of conformations. All of the chains are loosely attached to a planar ($Z = 0$ in an arbitrary Cartesian coordinate systems) interface. The head of every chain can move in the X and Y directions; however, a marginally small excursion (by the distance $+1$) from the $Z = 0$ plane is also allowed. This negligible thickness of the absorption surface is necessary in order to make the motion of the lattice chains physically possible.

The dimensions of the Monte Carlo box are $L_x \times L_y \times L_z$ with $L_x = L_y = L$. The value of L_z is sufficiently large enough to accommodate the $n = 17$ chain, even in its most extended conformation. There are superimposed periodic boundaries in the X and Y directions, and every chain leaving the MC box on one side wall is at the same time entering the box on the opposite wall. Therefore, the system represents a virtually infinite layer of terminally attached chains. Recognizing the periodicity of the configuration, the surface packing density may then be defined as $\rho = N/(L^2/8)$. The factor of 1/8 emerges from the assumed integer representation of the diamond lattice points. Here $\rho = 1$ corresponds to the close packing of the chain heads on the interface, and consequently, the close packing of the chain segments in the entire layer. The idea of the MC box used in these simulations is presented in Fig. 1.

The model of the chain dynamics consists of the following set of elementary conformational rearrangements. First, there are the three bond, two bead, kink motions.[6] This involves a simple permutation of two bond vectors separated by a third vector. The chain ends (head segments, as well as tail segments) need to be treated differently; their motion involves a two-bond, end jump.[6] Single bond end jumps are also allowed. The third type of elementary motion is the very small distance slithering of the entire molecule down the chain contour in a randomly selected direction. This is realized by adding a new segment on one end of the chain and clipping-off one segment on the opposite end, provided that the distance of the chain head from the impenetrable interface remains 0 or 1. These reptation-like moves are attempted with a frequency of $1/n$, with respect to the frequency of the two-bead kinks. The above scaling roughly acounts for the assumption of a uniform friction constant per chain

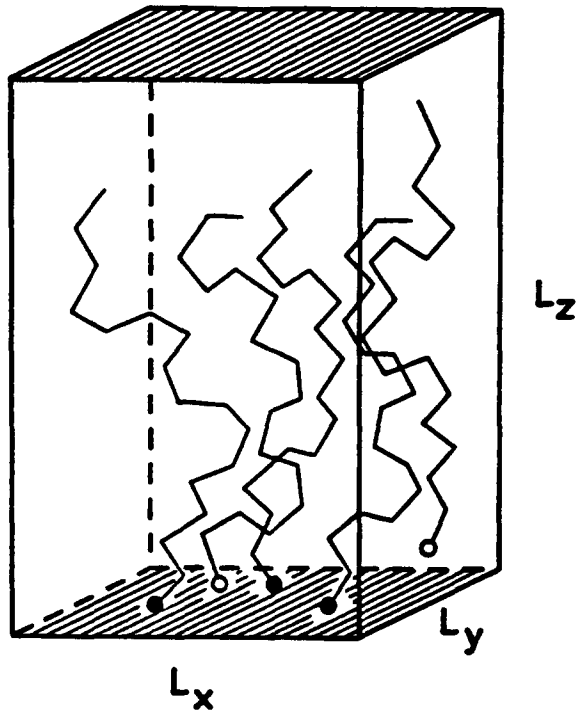

FIG. 1. Schematic representation of the Monte Carlo box. The shaded walls are impenetrable. The solid circles represent the chain head on a $Z = 0$ plane, and the open ones, the head at $Z = 1$. See the text for more details.

bead. More complicated models of dynamics, including, for example, four-bond rearrangements were also tested. These have only a marginal effect on the dynamics due to the high density, the local nematic type of ordering of the chain segments and the small chain length. Under these conditions, the relaxation of the chain conformation by four-bond motions is much less frequent than by the propagation of the three-bond kinks. A more detailed discussion of the problem can be found elsewhere.[12a,12b]

The time unit is defined as the time necessary for $N*n$ attempts at kink jumps plus N attempts at reptation steps. The sequence of elementary motions and their location (the chain index and the bead number in the case of kink) are carefully randomized.

Systems at various densities were studied. In each case, the initial configuration has been equilibrated by a sufficiently long run. Then, the results of MCD production runs are used to study the static and dynamic properties of the system. The average values of these properties are obtained by both ensemble and time averaging.

III. RESULTS AND DISCUSSION

A. Static properties

Five systems, at various surface densities of the chain molecules were studied in this work. Table I, columns 2 and 3, contains the description of the size of these systems. For easy reference in the remainder of this work, the surface density is used as a label for the system under the consideration. Several equilibrium properties of the model systems were measured in order to analyze the effect of density on the conformation of a single chain and consequently, on the distribution of the chain segments across the layer.

TABLE I. Summary of properties.

ρ	N	L	D MCD	D Eq. (7)	τ MCD	τ Eq. (9)
0.2	10	20	0.54(±0.02)	0.540	10.0	10.0
0.375	12	16	0.31(±0.01)	0.311	15.0	13.3
0.5	16	16	0.14(±0.02)	0.140	19.0	21.5
0.625	20	16	0.04	0.040	50.0	49.2
0.75	24	16	0.005	0.007	175.0	175.1

A comparison of the numerical values of the self-diffusion coefficient, D, and the relaxation time, τ, of the parallel to the interface component of the head-to-tail vector for various surface densities, ρ, in arbitrary units.

In some sense, the equilibrium properties of this system are related to those of a polymer brush, except that in a brush one of the chain ends are grafted to the surface, and here both ends of the chain are mobile. Thus, we shall compare the equilibrium results obtained from these simulations with extant polymer brush theories of Alexander[22] and Milner *et al.*[23]

The thickness of the model monolayer depends upon the surface density of the chains. It may be characterized by the average distance of the chain tail bead from the interface $\langle R_\perp \rangle$. As seen in Fig. 2, $\langle R_\perp \rangle$ at high densities increases linearly as $\rho^{1/3}$, in agreement with the scaling theory of Alexander[22] and the SCF theory of Milner *et al.* Similar behavior has been observed in a molecular dynamics simulation of polymer brushes by Murat and Grest,[24,25] who find a linear regime when $N\rho^{1/3} \geqslant 15$. Here, the linear regime occurs for $N\rho^{1/3} \gtrsim 14$. The conformation of the chains tends to be more extended for high density. Simultaneously, this increases the orientational order of the chain segments, and consequently, the orientational order of the entire chain. Let us define the angle between the end-to-end vectors of a pair of chains.

$$\cos(\gamma) = (\mathbf{r}_i \cdot \mathbf{r}_j)/(|\mathbf{r}_i| \cdot |\mathbf{r}_j|), \tag{1}$$

where $\mathbf{r}_i$ is the vector from head to tail of the ith chain. Then, the following-order parameter may be calculated:

$$s_r = [3\langle \cos^2(\gamma) \rangle - 1]/2, \tag{2}$$

with $\langle \cos^2(\gamma) \rangle$ computed as an ensemble average.

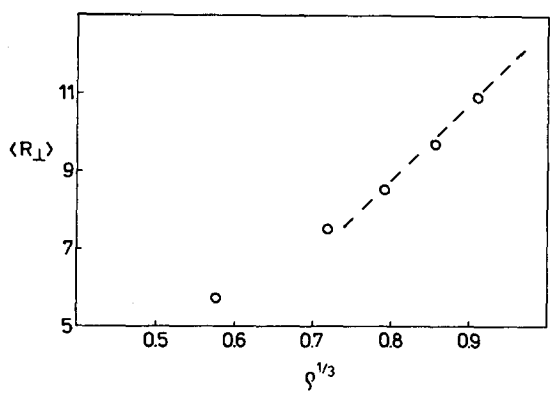

FIG. 2. Plot of the average distance of the chain tail from interface, as a function of the surface density $\rho^{1/3}$. The open circles represent the simulation data. The line is an arbitrary interpolation.

Figure 3(a) shows the dependence of s_r on the surface density ρ. One can see that the increase of ρ from 0.2 to 0.75 is accompanied by the increase of the order parameter s_r, from the value close to zero, characteristic of a random orientation, up to a value in the range of 0.4, which indicates that substantial ordering of the system has occurred. On a more local level, it is useful to consider the angle, β, between the bond vectors and the orthogonal to the surface. Due to the lattice representation, pairs of bond vectors are used in order to describe the orientation of the chain segment. Then, the following-order parameter defines the degree of the layer ordering as a function of distance from the chain head:

$$s_k = [3\langle \cos^2 \beta \rangle - 1]/2. \tag{3}$$

This quantity is dependent not only upon density ρ, but also on the position down the chain (k is the segment number counted from the head to the tail). In Fig. 3(b), s_k profiles are plotted for various values of the surface density ρ. These curves are in qualitative agreement with NMR data for the phospholipid bilayer.[26–28] Murat and Grest[24,25] have calcu-

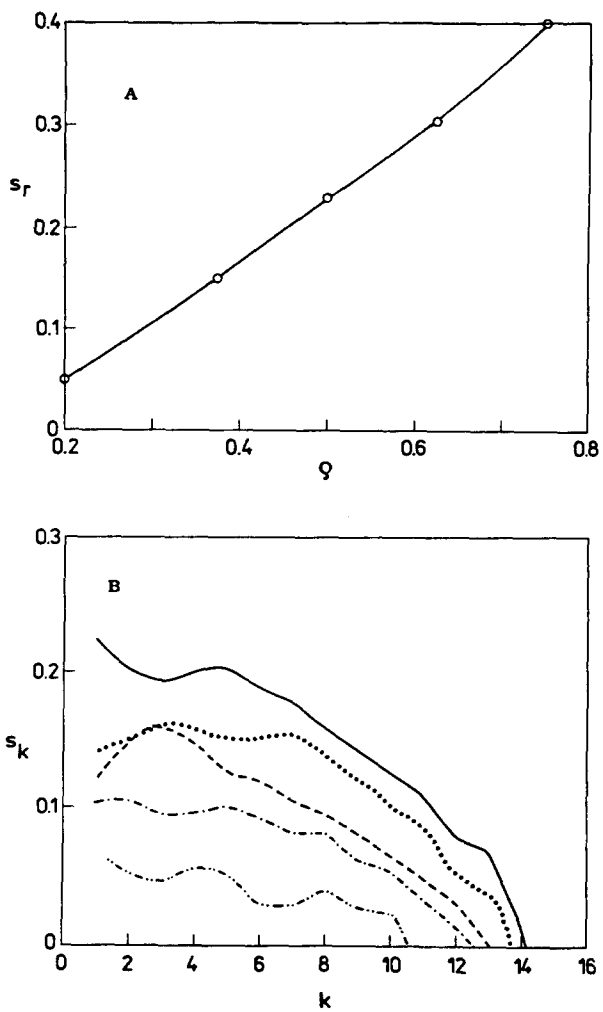

FIG. 3. (a) Plot of the order of parameter s_r for head-to-tail vectors [Eq. (2)] versus surface density ρ. (b) Plots of the order parameter s_k for the k th chain segment versus k (counted from the interface). The curves are arbitrary interpolations through the MCD data for $\rho = 0.75$ (top), $\rho = 0.625$, $\rho = 0.5$, $\rho = 0.375$, and $\rho = 0.2$ (bottom).

lated a quantity that is related to $\langle \cos\beta \rangle$, which exhibits qualitatively similar behavior at high density as Fig. 3(b). Due to the fact that here the ends are mobile and in the Murat–Grest simulation they are pinned, differences between the two simulations are seen at low densities. Murat and Grest observe a monotonic increase the closer one gets to the wall; here, oscillatory behavior is observed.

The curve for $\rho = 0.75$ is actually in quantitative agreement with Brown and Williams' [3] compilation of various NMR data for membranes in which the alkane chains contain $n = 16$ carbon atoms; i.e., the close, real equivalent of the present model.

Next, let us consider the segment density in the model monolayer, as a function of the distance from interface. The Alexander scaling theory[22] assumed a uniform density profile, while the SCF approach predicts a parabolic surface. For ease of comparison between the various profiles, the data are normalized by $\tilde{\rho}_z = \rho_z/(n*\rho)$, where ρ_z is the average segment density (the fraction of the lattice sites occupied by the polymer beads) at the distance z from the interface. Figures 4(a) and 4(b) present plots of $\tilde{\rho}$ as a function of $(z/\rho)^2$. At lower densities, these plots are qualitatively similar to those of Murat and Grest[24,25] and provide support for a parabolic density profile, as predicted by Milner *et al.*[23] At higher density, in particular at $\rho = 0.75$, the density profiles are decidedly nonparabolic.

The above brief analysis shows that the equilibrium properties of our model system are in quite close agreement with the properties of the corresponding real physical systems and exhibit similar equilibrium features as polymer brushes.[22,23] In spite of some simplifications discussed in previous sections of this paper, there is also good agreement with theory. In the next section, we discuss the dynamic behavior of the model.

B. Dynamic properties

The dynamic properties of the model system can be characterized by the behavior of various autocorrelation functions. Let us consider, as an example, the center-of-mass autocorrelation function of a single chain. This is the mean-square displacement of the chain center of mass as a function of time given by

$$g_{\text{c.m.}}(t) = \langle [\mathbf{r}_{\text{c.m.}}(t) - \mathbf{r}_{\text{c.m.}}(0)]^2 \rangle, \tag{4}$$

where $\mathbf{r}_{\text{c.m.}}(t)$ is the center of gravity coordinate at time t, and all averages are corrected for the center-of-mass displacements of the entire collection of chains.

To further examine the character of the chain dynamics, the single bead autocorrelation functions were computed for the following parts of the chain:

(i) $g_m(t)$, the mean-square displacement of the three central beads of the chain, (ii) $g_h(t)$, the mean-square displacement of the chain head (the beads that move on the interface), and (iii) $g_e(t)$, the mean-square displacement of the chain tail. In all of these cases, the motion of the center of mass of the entire system has been subtracted, as was done for $g_{\text{c.m.}}$.

In Fig. 5, $g_{\text{c.m.}}(t)/t$ is plotted versus time for various surface densities ρ. At long times, a plateau is reached, and the value of this plateau divided by 6 gives the self-diffusion constant. Standard free-diffusion behavior is recovered at long times. Numerical values of D, together with the values of 90% confidence limits (when available), are compiled in Table I.

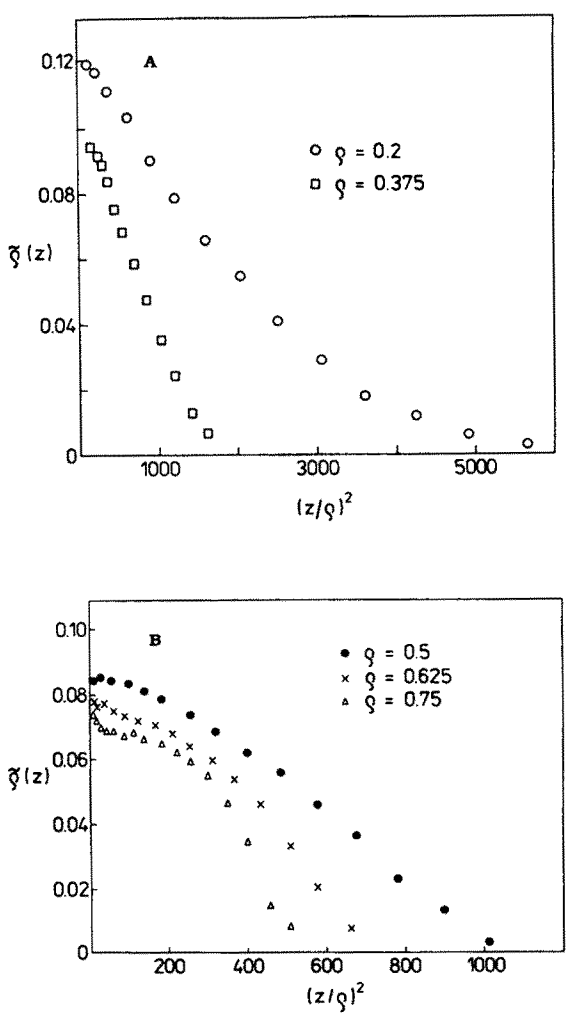

FIG. 4. Profiles of the density of the chain segments in the model layer versus $(z/\rho)^2$, with z as the distance from the surface. (a) The open circles are for $\rho = 0.2$ and the squares are for $\rho = 0.375$. (b) The solid circles are for $\rho = 0.5$, the crosses are for $\rho = 0.625$, and the triangles are for $\rho = 0.75$.

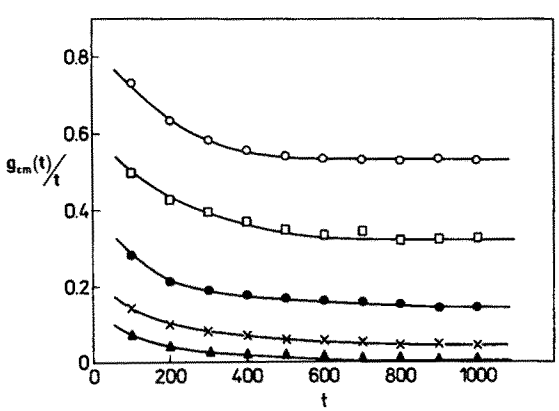

FIG. 5. Plots of mean-square displacement of the center-of-mass of the chain divided by time, $g_{\text{c.m.}}(t)/t$, versus time, t, for various values of ρ. The lines are arbitrary interpolations of the simulation data.

Is this dependence similar to that seen for the polymer solutions?[29] To answer this question, the D data have been fitted by

$$D = D_0 \exp(-a\rho^{v}), \tag{5}$$

where a and v are adjustable parameters. Here D_0 can be considered either as the value of the self-diffusion coefficient at the infinite dilution or as an adjustable parameter. The fitting procedure gives $D_0 = 0.981$, $a = 6.09$, and $v = 2.73$. The values of D calculated from Eq. (5) with these parameters are also given in Table I for comparison. The fit is of rather good quality. The value of v obtained is larger than typical values (1/2–1) for polymer solutions,[29] and consequently, the self-diffusion coefficient exhibits a stronger dependence upon the density than is usually observed for polymer solutions.

Next, let us consider the motion of different parts of the chain. In Fig. 6, the autocorrelation functions for the chain head, the middle part of the chain, and the chain tail are plotted against time for the case of $\rho = 0.2$. There is a clear difference between the short time (and distance) mobility of chain segments at different positions down the chain. As expected, the most mobile are the tail segments. The lowest mobility is exhibited in the middle section of the chain. Faster, short distance motion of the chain ends is typical for polymer solutions and melts.[12b] Here, this phenomenon is seen in systems with quite different restrictions on the dynamics. This suggests that the short time dynamics may be rather similar. The somewhat slower motion of the chain head, when compared with the tail, may be caused by the restriction of the head displacements to the vicinity of the planar interface. This restriction slows down the motion of the rest of the chain at relatively long times. Eventually, all parts of the chain move with the same long-time self-diffusion coefficient—all the curves in Fig. 6 coincide. Their coalescence takes place after times when the memory of the chains' initial conformation disappears. The increase of surface density slightly changes the above picture. For larger values of ρ, the tail motion still dominates, and the short distance mobility of the head segments becomes closer to the motion of the middle segments. The effect is most likely related to the increase of the orientational order of the chain segments in denser systems, which is dependent on the distance from the interface. The more disordered tail side of the layer exhibits higher mobility at short times, and the motion is less cooperative for the tail segments.

It is interesting to analyze in more detail the various time regimes of the chain dynamics. For the sake of clarity, the simulation data for the tail segments autocorrelation function of the $\rho = 0.2$ case are plotted separately in Fig. 7. It is clear that prior to free diffusion (long distance) motion, which is characterized by $g_e(t) \sim t^1$ dependence, there is a broad range of times and distances where the motion is strongly hindered. At very short times, which corresponds to the displacement of the chain beads over the range of the average distance between the closest pair of chains, the motion is characterized by an autocorrelation function roughly proportional to $t^{1/2}$. This is typical for every kind of flexible molecule; with a $t^{1/2}$ predicted by the classical Rouse model of chain dynamics.[12] Then, there is a time regime of even more restricted motion, which is quite well described by a $g(t) \sim t^{1/4}$ dependence (we have drawn straight lines of various slopes in Fig. 7 to make the comparison convenient for the reader). This range of segment dynamics can be viewed as a motion of chain fragments between obstacles superimposed by other chains. Finally, these obstacles disappear, since the chains in the system eventually move. This disengagement process presumably corresponds to the second $t^{1/2}$ regime or the crossover to the t^1 regime. A t^1 regime means that the memory of the initial conformation is already forgotten, and the free-diffusion limit is recovered. Figure 8 shows for the same times, the center-of-mass motions in which two distinguishable regimes can be observed. The first one, where $g_{\text{c.m.}} \sim t^{1/2}$, strictly corresponds to the entire range of hindered motion of an individual segment. The second one, the $g_{\text{c.m.}} \sim t^1$ regime, begins at the same time when $g_e \sim t$, as it should.

Very similar behavior can be seen for other parts of the chain, as well as for the systems of higher density. The only difference is in the width of the various regimes. As it might be expected, a higher surface density ρ leads to stronger restrictions on the local dynamics. In Fig. 9, one can see that

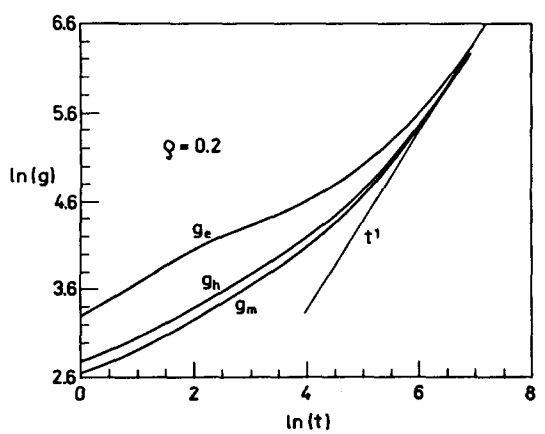

FIG. 6. Log–log plots of the single-bead autocorrelation function versus time for $\rho = 0.2$. Here g_e, chain tail, g_h, chain head; and g_m, average for the three middle beads. The straight line represents free diffusional motion.

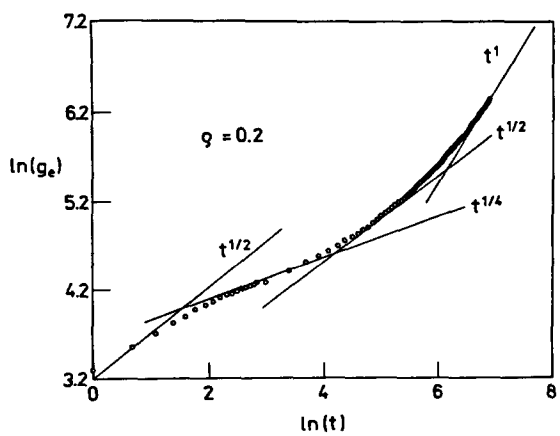

FIG. 7. Detailed log–log plot of the single-bead autocorrelation function g_e versus time t for $\rho = 0.2$. The circles represent simulation data. See comments in the text.

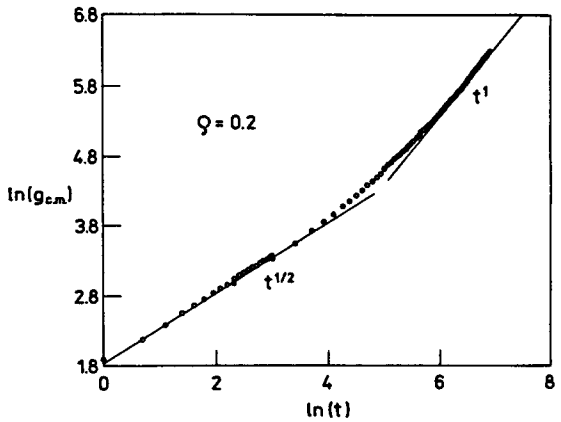

FIG. 8. Log–log plot of chain center-of-mass autocorrelation function $g_{c.m.}$ versus time t for $\rho = 0.2$.

the $g_c \sim t^{1/4}$ regime lasts for a significantly longer time for $\rho = 0.625$, than was seen for $\rho = 0.2$.

The above interpretation of the autocorrelation functions of the model system is, of course, somewhat speculative; however, it is consistent with all the simulation data. There is a striking similarity between the plots given in Figs. 7–9, and the results of theoretical[10,31] and computational[10–12] studies of dense polymer solutions and melts of long flexible polymers where chain entanglements become important. According to various criteria of entanglement onset for polymer systems,[10,30] the chains in our model layer are not entangled, at all. This is due to both the small chain length and the considerable orientational ordering in the system. The restrictions on chain dynamics in the layer are of a different origin. Among the most important are (1) the restriction of the head motion to the planar interface, with the concomitant strongly hindered relaxation of the orthogonal to the surface component of the chain dimensions and (2) the short-lived topological barriers. In other words, a rather different microscopic mechanism of system dynamics may lead to very similar observations, the best example of which is the behavior of the autocorrelation functions discussed above.

From the present MCD studies of a simplified model monolayer, the following picture of chain rearrangements and diffusion within the layer emerges. At very short times, the local dynamics is essentially indistinguishable from the dynamics of chain molecules in dense solutions or polymer melts. Then, the layer restrictions begin to control the chain dynamics. There is a relatively long waiting time when the chain finds itself in the cage created by surrounding, mostly parallel, chains. It is not an entanglement effect that slows down this intermediate distance motion. Rather, it is the highly cooperative relaxation of chain conformation and the interchange of position of two, or more likely several, chains which allows longer distance motion. Finally, the chain finds itself a new conformation and a new environment. This signals the onset of free lateral diffusion regime.

Note that the chain tails are more mobile than the chain heads over the entire intermediate time regime. This is due to "waving" of the chain portions on the more disordered, open side of the layer. This waving effect may be measured by the relaxation of the parallel to the surface component, of the head-to-tail vector. This can be described by the following autocorrelation function:

$$g_{r\|}(t) = \langle \mathbf{r}_{\|}(t)\cdot\mathbf{r}_{\|}(0)\rangle / \langle \mathbf{r}^2_{\|}\rangle. \tag{6}$$

Plots of $g_{r\|}$ versus time t are compared in Fig. 10 for various values of ρ. Unlike in polymer melt systems, a much broader spectrum of relaxation times is present. There is no simple, single exponential regime in the relaxation curves. Consequently, there is no leading, longest characteristic relaxation time. An average relaxation time τ may be defined as a time at which $g_{r\|}$ decays to the value equal to $1/e$ of the initial value. The resulting values of τ are given in Table I.

$$\tau = \tau_0 \exp(b\rho^{\mu}). \tag{8}$$

The dependence of τ on ρ can be fitted by Eq. (8) with $\tau_0 = 9.54$, $b = 7.19$, and $\mu = 3.15$. Apparently, there is no simple correlation between changes of τ and the self-diffusion coefficient D, with increasing density ρ. However, the width of the $t^{1/4}$ regime of the tail motion is roughly proportional to τ. The stretched exponential scaling dependence of the various autocorrelation functions can be related by a generalization of the coupling models of Ngai.[31]

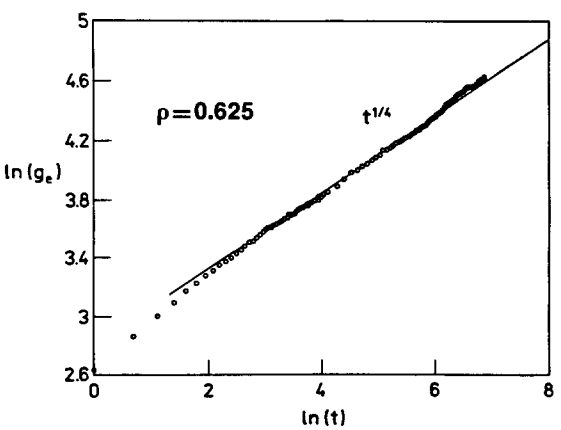

FIG. 9. Log–log plot of g_c vs t for the case of $\rho = 0.625$.

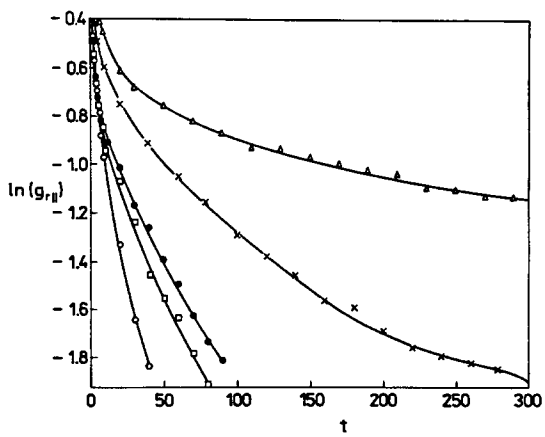

FIG. 10. Plot of the $\ln(g_{r\|})$ versus time for various surface densities. The triangles present MCD data for $\rho = 0.75$; crosses, $\rho = 0.625$; solid circles, $\rho = 0.5$; squares, $\rho = 0.375$; and open circles, $\rho = 0.2$. The lines represent an arbitrary interpolation through the data.

IV. CONCLUSION

The simplified lattice model of a monolayer of chain molecules terminally joined to an interface, may be considered as a crude model of the configuration of chain detergents, lipid bilayers, and related systems. In spite of the simplifications employed, the measured equilibrium properties of the model are in surprisingly good agreement with theoretical predictions,[23] with computer simulations of more detailed models[24,25] and for the equilibrium properties, with a computer simulation of grafted polymer brushes[24,25] and with experiments on real systems.[3,26–28] The short time dynamics of the model also agree with the related molecular dynamics and Brownian dynamics simulations[20,21] on membrane models. Therefore, there is reason to believe that the picture of longer time and distance dynamics which emerges from present simulations is relevant to the dynamics of the corresponding real systems.

It has been shown that the tails of the model chains, which correspond to the nonpolar alkane (alkene) chains of real systems are more mobile then the rest of the molecule. The mobility of the entire chain depends upon the degree of orientational ordering of the layer, which is an increasing function of surface density. After relatively long times associated with local wiggling of the chain, cooperative rearrangements of the chain position in the layer can be observed. This is then followed by lateral diffusion over long distances. Long distance diffusional motion is even more strongly dependent upon system density than is the local mobility.

The present model was not designed to study large distance motions of entire layers. This will be done in future work, which is in progress. There, a much more detailed model of a self-assembling lipid bilayer will be presented.

ACKNOWLEDGMENTS

A. Kolinski and M. Milik acknowledge the support of the Polish Academy of Sciences (CPBR 3.20). This research was also supported in part by the Polymer Program of the National Science Foundation.

[1] H. D. Napper, *Polymeric Stabilization of Colloidal Dispersions* (Academic, London, 1983).
[2] L. L. Randall and S. J. S. Hardy, Microbiology Rev. **48**, 290 (1984).
[3] M. F. Brown and G. D. Williams, J. Biochem. Biophys. Met. **11**, 71 (1985).
[4] V. Luzzati, in *Biological Membranes* (Academic, New York, 1968), pp. 71–123.
[5] P. J. Flory, *Statistical Mechanics of Chain Molecules* (Wiley, New York, 1969).
[6] A. Baumgartner, in *Applications of the Monte Carlo Method in Statistical Physics* (Springer, Heidelberg, 1984).
[7] K. Kremer, A. Baumgartner, and K. Binder, J. Phys. A **15**, 2879 (1981).
[8] A. Kolinski, J. Skolnick, and R. Yaris, J. Chem. Phys. **85**, 3585 (1986).
[9] A. Kolinski, J. Skolnick, and R. Yaris, Macromolecules **19**, 2550 (1986).
[10] J. Skolnick and A. Kolinski, Adv. Chem. Phys. (in press).
[11] K. Kremer, Macromolecules **16**, 1632 (1983).
[12] A. Kolinski, J. Skolnick, and R. Yaris, J. Chem. Phys. (a) **84**, 1922 (1986); (b) **86**, 1567 (1987); (c) **86**, 7164 (1987).
[13] E. Eisenrigler, K. Kremer, and K. Binder, J. Chem. Phys. **77**, 6296 (1982).
[14] M. Milik and A. Orszagh, (a) Polymer **30**, 681 (1989); (b) Polymer **31**, 506 (1990).
[15] S. Livne and H. Meirovitch, J. Chem. Phys. **88**, 4498 (1988).
[16] H. Meirovitch and S. Livne, J. Chem. Phys. **88**, 4507 (1988).
[17] M. Lal and R. J. Stepto, J. Polym. Sci. Polym. Symp. **61**, 401 (1977).
[18] C. A. Croxton, J. Phys. A **19**, 987 (1986).
[19] C. A. Croxton, Polym. Commun. **28**, 57 (1987).
[20] P. G. Khalatur, A. S. Pavlov, and N. K. Balabaev, Macromol. Chem. **188**, 3029 (1987).
[21] R. W. Pastor, R. M. Venable, and M. Karplus, J. Chem. Phys. **89**, 1112 (1988).
[22] S. J. Alexander, J. Phys. Paris **38**, 983 (1977).
[23] S. T. Milner, T. A. Witten, and M. E. Cates, Europhys. Lett. **5**, 413 (1988); Macromolecules **21**, 2610 (1988); S. T. Milner, Europhys. Lett. **7**, 695 (1988).
[24] M. Murat and G. S. Grest, Phys. Rev. Lett. **63**, 1074 (1989).
[25] M. Murat and G. S. Grest, Macromolecules **22**, 4054 (1989).
[26] J. Seelig and A. Seelig, Q. Rev. Biophys. **13**, 19 (1980).
[27] M. F. Brown and J. Seelig, Bio. Chem. **17**, 381 (1978).
[28] M. F. Brown, J. Seelig, and V. Haeberlen, J. Chem. Phys. **70**, 5045 (1979).
[29] G. D. J. Phillies, Macromolecules **19**, 2367 (1986).
[30] P. G. de Gennes, *Scaling Concepts in Polymer Physics* (Cornell University, Ithaca, New York, 1979).
[31] K. L. Ngai and J. Skolnick, J. Chem. Phys. (to be submitted).